Materials for Renewable and Sustainable Energy (2022) 11:105–114
https://doi.org/10.1007/s40243-022-00210-7

ORIGINAL PAPER

Copper nanoparticles suitable for bifunctional cholesterol oxidation reaction: harvesting energy and sensor

F. I. Espinosa-Lagunes[1] · J. C. Cruz[2] · R. E. Vega-Azamar[2] · I. Murillo-Borbonio[4] · Julieta Torres-González[1] · Ricardo A. Escalona-Villalpando[4] · M. P. Gurrola[3] · J. Ledesma-García[4] · L. G. Arriaga[1]

Received: 16 March 2022 / Accepted: 25 May 2022 / Published online: 21 June 2022

Abstract

This study reports the performance of simple low-cost synthesized bifunctional Cu/Cu_2O nanoparticles (NPs) used as a catalyst for energy-harvesting applications through of a microfluidic fuel cell (μFC), and further, as cholesterol (Chol) sensor. TEM characterization of the NPs showed spheres between 4 and 10 nm, while XRD and XPS analysis confirmed the composition and preferential crystallographic plane of Cu/Cu_2O. In addition, 25.26 $m^2\ g^{-1}$ surface area was obtained, which is greater than those commercial materials. NPs showed high activity toward the cholesterol oxidation reaction when were used as a sensor, obtaining a linear interval between 0.5 and 1 mM and 850 μA $mM^{-1}\ mg^{-1}$ of sensitivity and 8.9 μM limit of quantification LOQ. These values are comparable to results previously reported. Moreover, Cu/Cu_2O NPs were used as anode in a μFC with 0.96 V of cell voltage and 6.5 mA cm^{-2} and 1.03 mW cm^{-2} of current and power density, respectively. This performance is the highest currently reported for cholesterol application as an alternative fuel, and the first one reported for a microfluidic fuel cell system as far as is known. Results showed that the obtained Cu-based NPs presented an excellent performance for the dual application both μFC and sensor, which has potential applications in biomedicine and as an alternative energy source.

Keywords Cholesterol oxidation reaction · Cu/Cu_2O nanospheres · Cholesterol sensor · Bifunctional Cu-based catalyst · Microfluidic fuel cell

Introduction

The search for new energy sources has been at the center of research efforts in the last decade, and electrochemical systems are an excellent option because they exceed the efficiency of those based on the Carnot principle [1, 2]. In this sense, a novel electrochemical coupling is possible due to the development of devices such as the microfluidic fuel cell (μFC), which are compatible with organic, microbiological, enzymatic, and inorganic electrodes, thus being applicable in biomedicine as a power supply for biosensors and even as an analytical sensing system used in microchips [3, 4]. μFC operation consists of the fuel and oxidant separation by laminar flow without the need of a physical barrier, such as a membrane, allowing an excellent ionic transport. Consequently, one of the main problems of these microfluidic devices is the electrodes composition and the flow through them. On the other hand, one of the most important advantages is that different fuels can be used to produce energy and be quantified; fuels such as glucose, ethanol, methanol

✉ M. P. Gurrola
mayra.pg@chetumal.tecnm.mx

Ricardo A. Escalona-Villalpando
ricardo.escalona@uaq.edu.mx

1 Centro de Investigación y Desarrollo Tecnológico en Electroquímica, 76703 Pedro Escobedo, QRO, México

2 Tecnológico Nacional de México, Instituto Tecnológico de Chetumal, Av. Insurgentes 330, David Gustavo Gutiérrez, 77013 Chetumal, Q ROO, México

3 CONACYT-Tecnológico Nacional de México/Instituto Tecnológico de Chetumal, Av. Insurgentes 330, 77013 Chetumal, Q ROO, México

4 División de Investigación y Posgrado, Facultad de Ingeniería, Universidad Autónoma de Querétaro, 76010 Querétaro, QRO, Mexico

and glycerol have been reported [5, 6]. One molecule that has received few attention as a fuel in studies is cholesterol, although it is of high biomedical interest for the continuous control of cholesterol in blood serum to minimize the risk of cardiovascular diseases [7].

Beyond the scope of μFCs, research in self-powered sensors is currently focused on the development of options for the use of the current generated by the oxidation of cholesterol [8]. Specifically, for the oxidation of cholesterol (Chol) as a fuel, oxidase (ChOx) has been used, however, this enzyme tends to generate resistance to mass transfer, thus increasing activity loss [9, 10]. Therefore, the replacement of this enzyme by abiotic catalysts, such as Pt, Pd, Ir, Rh, Os, and Ru, has been considered since these inhibit the poisoning generated by secondary products in the oxidation of organic molecules [11–15]. Nevertheless, one of the main disadvantages of these materials is their high cost and the decrease in catalytic loads [16]. In this sense, different Ag electrocatalysts have been developed with several nanostructures and particle sizes between 1 and 10 nm, but an alternative material with a high potential to be used is Cu because it is inexpensive, excellent conductor, and highly selective for the oxidation of different organic molecules such as hydrocarbons, glucose, ascorbic acid, L-cysteine, uric acid, and dopamine [11, 17].

Therefore, Cu is a potential material to use as a catalyst in microfluidic systems as a μFC or sensor, since this material provides dual functionality: on the one hand, it can oxidize the fuel for energy production and, on the other hand, it can act as a functional material suitable to be used as an amperometric sensor [18]. In the literature, data on non-enzymatic cholesterol detection using several electrode systems are scarce; for example, it has been reported that electrodes based on carbon nanofibers nanocomposites/Cu/Ni-dispersed polymer, with a sensitivity of 226.2 μA mM^{-1} cm^{-2} and Cu_2S [19] nanoplates on Cu rods as a biosensor, reaching a sensitivity of 62.5 μA mM^{-1}, among others [20, 21]. In addition, the development of these materials has limitations, such as the way the incorporation into the electrodes affects cell morphology, active sites, and homogeneity, which are essential for the functionality of a μFC system [17, 22].

Thus, in this work, Cu/CuO_2 NPs with average particle sizes between 4 and 10 nm (smaller than previously reported) were synthesized as a bifunctional material for both as an electrochemical sensor in Chol oxidation and as a fuel in a μFC system in alkaline conditions [11]. For the case of Cu/CuO_2 NPs as a cholesterol sensor, results showed a linear range between 0.5 and 1 mM, 850 μA mM^{-1} mg^{-1} of sensitivity, and limit of detection LOD and quantification LOQ of 2.6 μM and 8.9 μM, respectively. These results indicate that the material works as a catalyst in the Chol oxidation reaction and that it is also possible to obtain the highest performance reported for a fuel cell using cholesterol as a fuel: the μFC registered a high voltage value (0.98 V), as well as a high current and power density of 6.5 mA cm^{-2} and 1.03 mA cm^{-2}, respectively, during the evaluation. These results allow to state that not only a material with potential for a dual application can be obtained, but also, to the best of our knowledge, to report the first μFC that uses cholesterol as fuel.

Experimental methodology

Chemicals

All chemicals were reagent grade, used without any further modification. Ethylene glycol was purchased from J.T. Baker (≥ 99.9%), polyvinylpyrrolidone (PVP, wt = 360,000), ascorbic acid (Macron ≥ 99%), acetone (J.T. Baker ≥ 98.5%), $CuSO_4$, J.T. Baker (≥ 98.5%), 18 MΩ cm deionized water. Cholesterol (SIGMA > 99%), NaOH (J.T. Baker > 97%), Toray carbon paper 060 (wet proofed), acetic acid (J.T. Baker ≥ 98.5%), Chitosan (SIGMA low molecular weight), KOH (J.T. Baker ≥ 97.5%) and Triton® X-100 (Hycel), Pt (40% CV/CX-3), and Nafion (SIGMA 5 wt. % in lower aliphatic alcohols and water, containing 15–20% water).

Cu/Cu_2O synthesis

Cu NPs were synthesized according to the modified core–shell Cu/Pd synthesis method reported by J. Maya-Cornejo et al. [23]. In a 100 mL round-bottom flask, ethylene glycol was added at 80 °C while stirring at 350 rpm. Subsequently, 6.6 g ascorbic acid and 1 g polyvinylpyrrolidone were added. After 30 min, 1 g $CuSO_4$ precursor salt was added and the reaction was left for 36 h, at constant temperature. After that, acetone and deionized water (DI) washes were performed, and a brown precipitate was observed. Finally, the precipitate was set to dry for 6 h at 60 °C.

Cu/Cu_2O physicochemical characterization

X-ray diffraction (XRD) measurement was carried out in a Bruker X-ray diffractometer (model PW3710). The preliminary study of the Cu NPs size, between each synthesis, was performed by light scattering dispersion (DLS) using a Zeta Sizer Nano Series Nano-ZS90 instrument at an angle of 173°. Scanning electron microscopy (SEM) with a JEOL brand microscope (JSM-6060 LV) was carried out, while surface mapping was performed with dispersive energy X-ray spectroscopy (EDS, BrukerXFlash 6110 detector). Physicochemical properties of the modified electrodes were investigated with a thermogravimetric analyzer 2950 TGA HR V5.5 TA in air, following the variation of the weight loss percentage, performed

between 25 and 800 °C, at 5 °C min^{-1} heating rate of with the incorporation of differential scanning calorimetry DSC technique. Textural properties of the modified electrodes were analyzed by N_2 adsorption–desorption isotherms at −196.15 °C using a Micromeritics TriStar 3000 equipment. Surface area was calculated according to the Brunauer–Emmett–Teller (BET) equation. X-ray photoelectron spectroscopy (XPS) analysis was used to establish the oxidation states of the synthesized Cu NPs using a Monochromatic Magics Thermo Scientifics instrument, model K-Alpha + in conditions of $v = 1$ scan min^{-1} in $t = 20.5$ s y CAE = 20.

Electrochemical characterization

Evaluation of Cu/Cu_2O as a cholesterol sensor

Preparation of the Cu/Cu_2O-based electrodes (working electrode) consisted in an ink previously prepared using 1 mg of Cu/Cu_2O NPs, 0.5% Chitosan (low molecular weight) w/w and 15% acetic acid. Then, 4 µL was deposited on Toray carbon paper (0.25 cm^2). The reference and the counter electrode were Ag/AgCl and a Pt wire, respectively. KOH (0.3 M) was used as electrolyte for the fuel cell and sensor. For the evaluation of the sensor, cyclic voltammetry was performed at 10 mV s^{-1} as scan rate in a potential range between −1 and 0.2 V (vs. Ag/AgCl) with different Chol concentrations (0.1–1 mM) using a Potentiostat/Galvanostat (Biologic VSP-0363). Sensitivity (*S*) was calculated from the cholesterol sensor calibration curve slope, while the limit of detection (LOD) is 3.3 σ/*S,* where σ is the standard deviation, and the limit of quantification (LOQ) was calculated from 10 σ/*S* [24–26]. All experiments were performed in triplicate and the standard deviation was reported.

Evaluation of Cu/Cu_2O NPs in a microfluidic fuel cell using cholesterol as a fuel

The µFC prototype used in this study has already been published by Escalona-Villalpando et al. [27]. The anode was prepared by deposition on a Toray paper electrode ($A = 0.25$ cm^2) 0.7 mg cm^{-2} of catalytic load of Cu/Cu_2O, along with 0.5% wt/wt Chitosan, 15% v/v acetic acid, and 15 mL was pipetted onto each carbon electrode surface. The anolyte consisted of 0.1 M KOH (Alyt > 97%) solution with 10% (w/w) Triton® X-100. The cathode was prepared by deposition of 1 mg of a mixture of 40% commercial Pt with a solution of 5% Nafion® and isopropanol via the spraying method proposed by Clicchio et al. in 2009 [28]; the catholyte consisted of 0.5 M H_2SO_4 solution. The polarization curve was linear at 10 mV s^{-1} sweep speed [24].

Results and discussion

Microscopy analysis

In Fig. 1a, the morphological analysis of Cu/Cu_2O NPs by transmission electron microscopy (TEM) is shown, where an average particle size between 6 and 7 nm can be observed, with 86% of the overall analyzed particles having a diameter between 4 and 10 nm, which is confirmed in the histogram (Fig. 1b) depicting particle size with respect to number of particles. In addition, a mapping through X-ray energy-dispersive spectroscopy analysis (Fig. 1c–f) displayed that Cu is uniformly distributed in the material, in addition to small amounts of oxygen, which can be attributed to the fact that irregular spheres are composed of Cu and CuO; the presence of C is associated to residual PVP from the synthesis process [19, 29]. This distribution is due to the synthesis method without using other materials such as reduced carbon oxide as a stabilizer [29].

Structural analysis by XRD and XPS

XRD analysis (Fig. 2a) shows the diffraction patterns of the Cu/Cu_2O materials, where the characteristic peaks were associated to the preferential crystallographic planes (1 1 1), (2 0 0) and (2 2 0), corresponding to the presence of Cu (JCPDS 04-0836) [30]. In addition, the planes (1 1 1), (2 0 0), (2 2 0) and (3 1 1) are related to Cu_2O (JCPDS 05-0667), suggesting the structure corresponds with Cu/Cu_2O [18, 31]. Scherrer equation was used to estimate the crystallite size for Cu^0 and Cu_2O, obtained an average size of 28 and 29 nm, respectively. The high-resolution XPS spectrum of the Cu 2*p* core level is displayed in Fig. 2b. Peaks for Cu 2*p*3/2 and Cu 2*p*1/2 correspond to a binding energy of 933.5 eV and 953.5 eV, respectively, which is according with the reported values of Cu^+ and oxidation state for Cu_2O [18, 32]. Satellite peaks indicate the existence of Cu^0 and Cu^{++}; the scanning signal (934.8 eV) corresponds to the Cu^{++} oxidation state attributed to the oxygen signal present in the EDS mapping. On the other hand, the first sweep (933.5 eV) is the response of Cu 2*p*. According to the analysis by deconvolution (using Advantage program, XPS Thermoscientific) 21 and 79 of atomic % correspond to Cu^{2+} and Cu^0, respectively. In addition, the spectroscopy presented in Fig. 2a was used to determine the interplanar distances, which was compared to those commercial NPs from Sigma-Aldrich (Table 1). This information exhibits an important closeness between the theoretical values (*) and those obtained for the synthesized Cu/Cu_2O NPs, with an error range not exceeding 9%, so it is possible that the material does not present structural modifications [33].

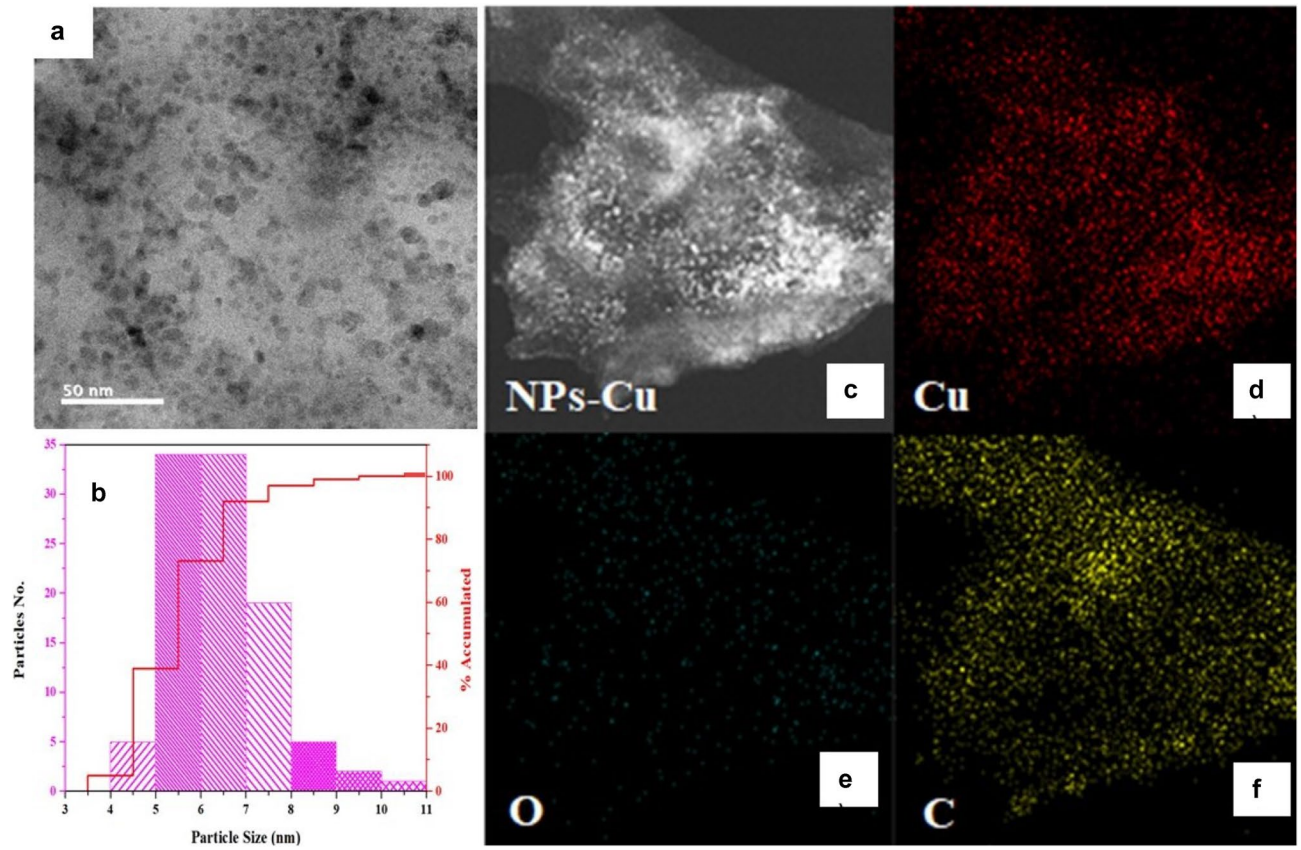

Fig. 1 **a** TEM morphological analysis of Cu/Cu_2O, **b** size distribution histogram, **c–f** EDS analysis of Cu/Cu_2O-based materials

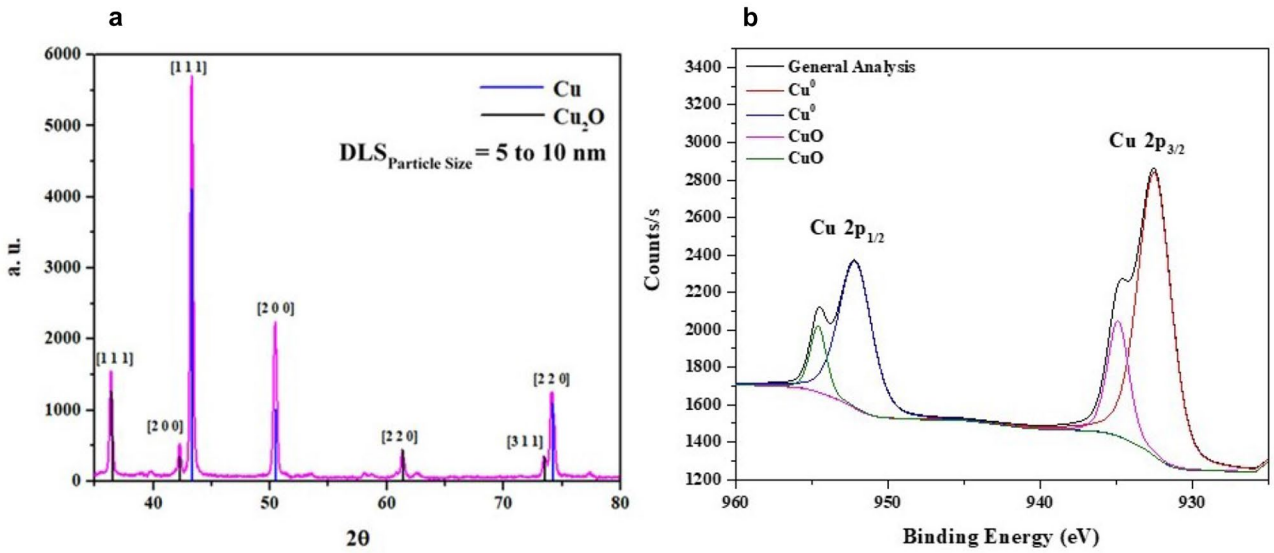

Fig. 2 **a** Diffractogram of Cu/Cu_2O, **b** photoelectric X-ray spectroscopy of Cu/Cu_2O

Table 1 Comparison of crystallographic parameters of synthesized NPs and commercial NPs

Material	2θ	Plane	Network parameter ($a^*=b^*=c^*$) (Å)	Network parameter ($a=b=c$) (Å)	Interplanar distance (d*) (Å)	Interplanar distance (d) (Å)
Cu	43.317	[1 1 1]	3.61	3.44	2.087	1.997
	50.449	[2 0 0]			1.807	1.806
	74.126	[2 2 0]			1.278	1.215
Cu_2O	36.441	[1 1 1]	4.26	4.34	2.463	2.478
	42.329	[2 0 0]			2.133	2.2
	52.488	[2 2 0]			1.508	1.539
Commercial Cu	42.156	[1 1 1]	3.58	3.35	2.087	1.997
	50.358	[2 0 0]			1.807	1.806
	73.987	[2 2 0]			1.278	1.215

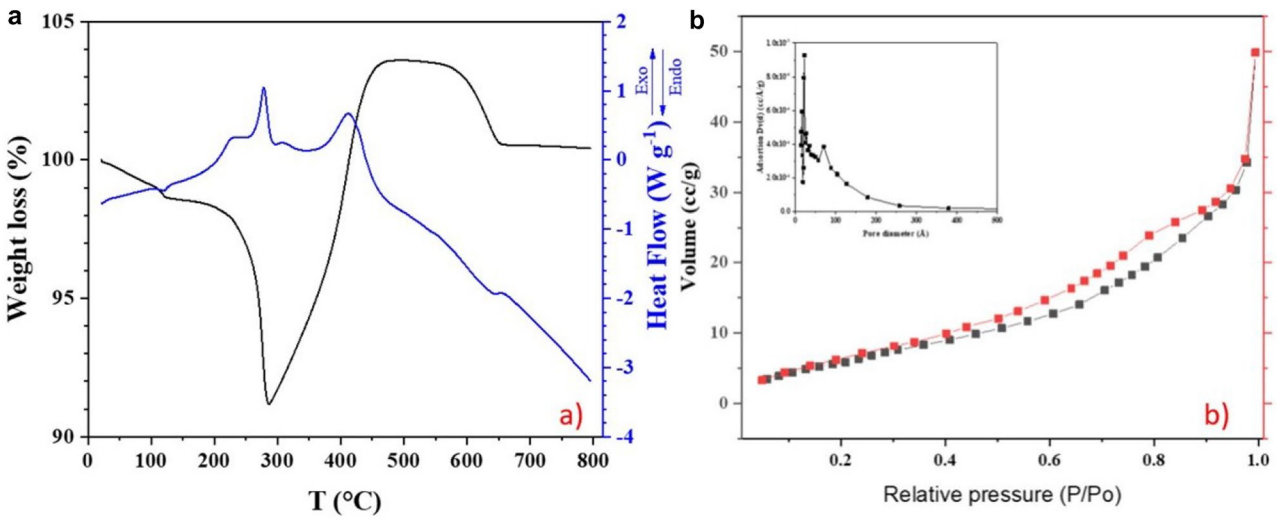

Fig. 3 **a** TGA–DSC s and **b** isothermal analysis of Cu/Cu_2O NPs

TGA–DSC analysis

In the TGA–DSC analysis of the Cu/Cu_2O NPs (Fig. 3a), a stable weight was observed as far as 107.1 °C; after that, the first degradation stage occurred with a loss of 2.34% of the overall weight, which is attributed to residual complexes from the initial synthesis. The resulting material degraded at 234 °C; then, the complex underwent a third stage of decomposition due to the loss of (C_6H_9NO) in Polyvinylpyrrolidone (PVP) molecule, with a weight loss of 8.4%, demonstrating an increase in the characteristic weight and the formation of new structures between carbonaceous material and transition metals. This complex decomposed until 472 °C, due to the loss of organic waste. Finally, the residue represents the weight corresponding to Cupric Oxide [34]. In addition, the isotherm corresponded to a Type IV, representative of mesoporous materials where the adsorption process involves the initial formation of a monolayer, increasing the relative pressure results in the formation of a multilayer (Fig. 3b).

This hysteresis cycle is associated to the filling and emptying of mesopores (pores with a size between 2 and 50 nm. Through BET analysis, the material's surface area was determined in 25.3 $m^2\ g^{-1}$, which compared to other authors is close to double the standard 14 $m^2\ g^{-1}$ for Cu/Cu_2O [35].

Electrochemical characterization

Evaluation of Cu/Cu_2O as cholesterol electrochemical sensor

The cyclic voltammetry (CV) of Cu/Cu_2O NPs on Toray carbon paper (TCP) displayed in Fig. 4a shows two oxidation peaks corresponding Cu to Cu^+ (−0.35 V) and Cu^{2+} (−0.03 V), respectively [22, 36, 37], in alkaline conditions. In addition, one reduction peak has been attributed

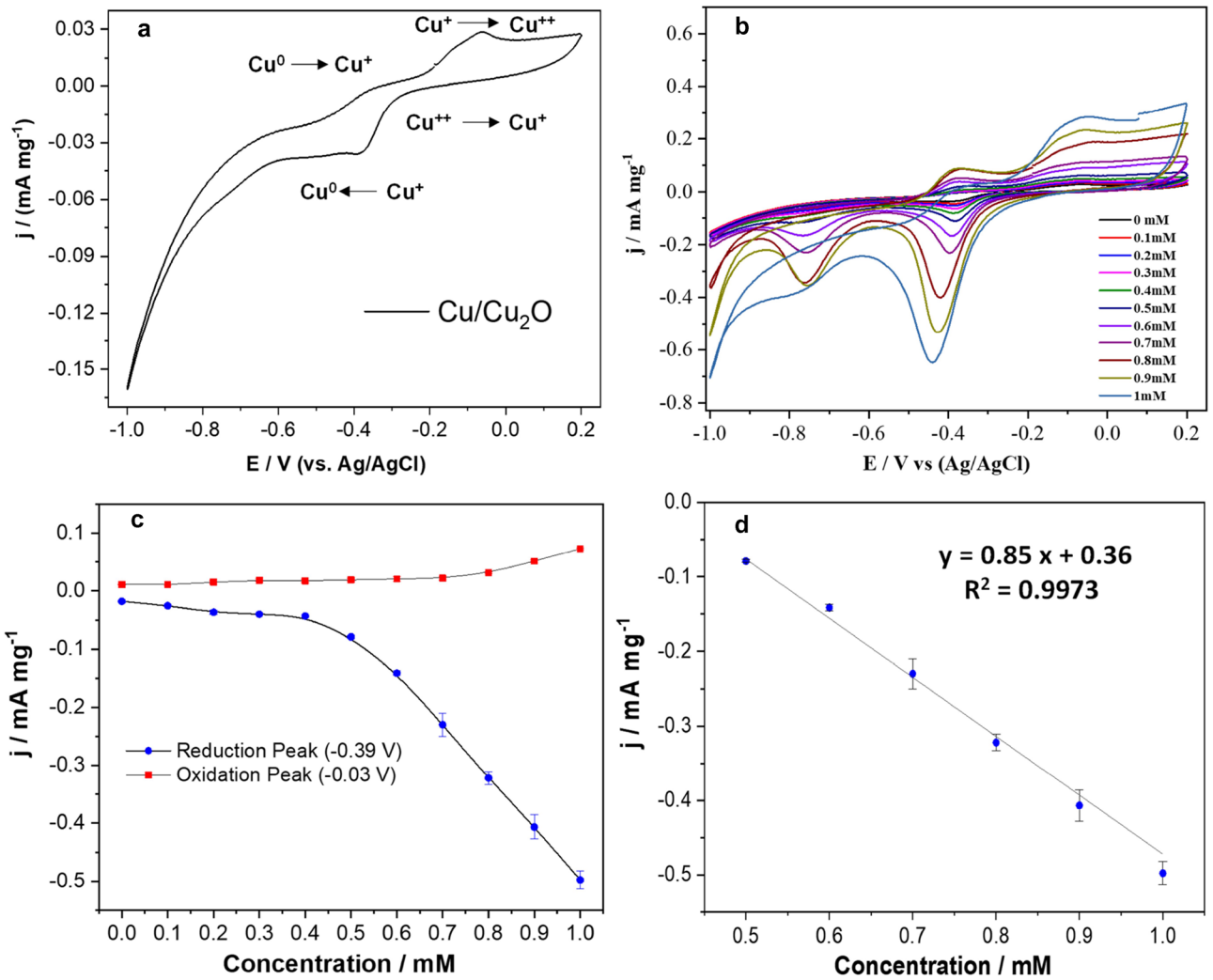

Fig. 4 **a** CV of Cu/Cu_2O in 0.1 M KOH in the absence of Chol at 10 mV s^{-1} scan rate; **b** CVs with additions of different concentrations of Chol (0–1 mM) in 0.1 M KOH; **c** calibration curve resulting from the analysis of the oxidation (−0.03 V) and reduction (−0.39 V) peaks; **d** linear range of reduction peak Chol addition (0.5–1 mM)

to the cathodic process of Cu^{2+} to Cu^{+} (−0.39 V), which is present in the mechanism for the Cu/Cu_2O redox reaction [18, 32, 38]. After that, Cu/Cu_2O NPs were evaluated in the presence of different cholesterol concentrations: from 0 to 1 mM (Fig. 4-b) observing an increase in the anodic current at −0.33 and −0.03 V (vs. Ag/AgCl) and cathodic peak at −0.34 V (vs. Ag/AgCl). In addition, the rise to a second reduction peak located at −0.75 V was observed. This redox process is attributed to the dependence of oxygen reduction on the Cu/Cu_2O crystal structure, which may be related to the Cu (II) complexion with molecule-forming soluble species according to Moelans et al., who reported this phenomenon for amino acids and other chelating agents such as S and O [39]. Subsequently, the oxidation (−0.03 V) and reduction (−0.39 V) peaks were analyzed for the sensor mode, because a higher increase in current density was observed (Fig. 4c), finding a higher sensitivity (850 µA mM^{-1} mg^{-1}) in a linear range of 0.5–1 mM ($R^2 = 0.9973$) for the reduction peak. As well as low limits of detection (LOD) and quantification (LOQ) of 2.6 and 8.9 µM, respectively (Fig. 4d). Already published results for non-enzymatic Chol sensors have been quite varied; for instance, Tong et al. reported a low linear range of 10–300 nM with an LOD of 1 nM using MWCNT and a molecularly imprinted polymer [40]. Yoshi and coworkers reported a higher linearity range of 1–20 mM (that is, within the range of cholesterol found in blood of 1.81–4.9 mmol/L) but a low sensitivity (8.08 µA mM^{-1} cm^{-2}) using Laponite–Montmorillonite material [41]. As for copper oxide materials, Khaliq et al. recently reported Cu_2O NP/TiO_2 nanotubes with a linear range of 24.4–622 µM, 0.05 µM of LOD, and 6034.04 µA mM^{-1} cm^{-2} sensitivity [18]. Results of the present study

are comparable with some of those mentioned above. The experimental strategy used for the evaluation of cholesterol, despite not being within the linear range found in real samples, is to dilute the sample and then multiply it by the dilution factor to obtain the final result to compare it with commercial cholesterol devices [18]. In other cases, multisensors that quantify cholesterol and other analytes such as uric acid, triglyceride and glucose have been reported [42, 43].

Evaluation of cholesterol as fuel in a μFC

The evaluation of the anode and cathode in a half-cell configuration was carried out under their respective experimental conditions. For the case of Cu/Cu_2O, 0.1 M KOH was used in the presence of 0.4 mM Chol (prepared as described above), obtaining an open circuit voltage OCV of $-0.13\ V \pm 0.05\ V$ (vs. Ag/AgCl); meanwhile the cathode was evaluated in 0.5 M H_2SO_4, reaching 0.74 ± 0.08 V (vs. Ag/AgCl) OCV. This result means that the fuel cell potential would be around 0.87 V, as shown in Fig. 5a. In the evaluation of the μFC, the independent anolyte and catholyte inlets were used to increase voltage, current, and power performance, while the flow rate was 3 mL h^{-1}, in accordance to previously reported works [27, 44, 45]. The current and power curves can be appreciated in Fig. 5b where, in the absence of fuel, the OCV was 0.38 ± 0.03 V and 0.34 ± 0.07 mA cm^{-2} of current density, showing a return in the curve, in the mass transfer region, which was expected in the absence of cholesterol. On the other hand, in the presence of 0.2 and 0.4 mM Chol, the OCV increased to around 0.65 ± 0.03 V, meanwhile the change in the current and power density was not significant: 0.76 ± 0.08 mA cm^{-2} and 0.12 ± 0.05 mW cm^{-2}, respectively. This behavior is very similar with respect to the evaluation of Cu/Cu_2O NPS as a cholesterol sensor, where no important change presented in current at these concentrations. With higher concentrations of cholesterol, the OCV increased from 0.79 ± 0.01 V to a maximum of 0.96 ± 0.02 V using 0.6 mM and 1 mM, respectively, while the current density increased 2.6 times (from 2.5 to 6.5 ± 0.09 mA cm^{-2}) and the power density by 2.3 times (from 0.44 to 1.03 ± 0.12 mW cm^{-2}). Similarly, this increased in the current behavior is observed in the same Chol concentrations when it was used as a sensor.

When comparing the results of this study to those previously published by another authors, it was interesting observe that there are only two studies reported for fuel cells using cholesterol. Minteer's team reported a cholesterol biofuel cell using the cholesterol enzyme dehydrogenase (ChDH) in the bioanode with the redox polymer $FcMe_2$-LPEI and the bilirubin enzyme oxidase (BOx) in the cathode linked to MWCNT-modified with anthracene, both in a single compartment. They reported 0.59 V OCV, 101 μA cm^{-2} and 20.3 μW cm^{-2} of current and power density respectively, at pH 7.5 and 5 mM Chol a of [46]. Sekretaryova reported a cholesterol self-powered biosensor using the enzyme cholesterol oxidase (ChOx) with phenothiazine in the anode and the enzyme ChOx with Prussian blue in the cathode; the cell had a single compartment and operated at pH 6.8 with 0.1 M KCl and 1% (w/w) Triton X-100 using different Chol concentrations. Although they reported 0.11 V OCV and 11.4 μW cm^{-2} power density; the focus of this work was the biosensor parameters [47]. In this context, it is interesting to analyze the results obtained for the current and power curves (Fig. 5b), where an apparently linear increase in OCV, current and power density can be observed, highlighting that, a $R^2 = 0.9915$ value in a linear range from 0.4 to 1 mM and 1.48 mW cm^{-2} mM^{-1} of sensitivity was obtained. These results suggest that this system can be used

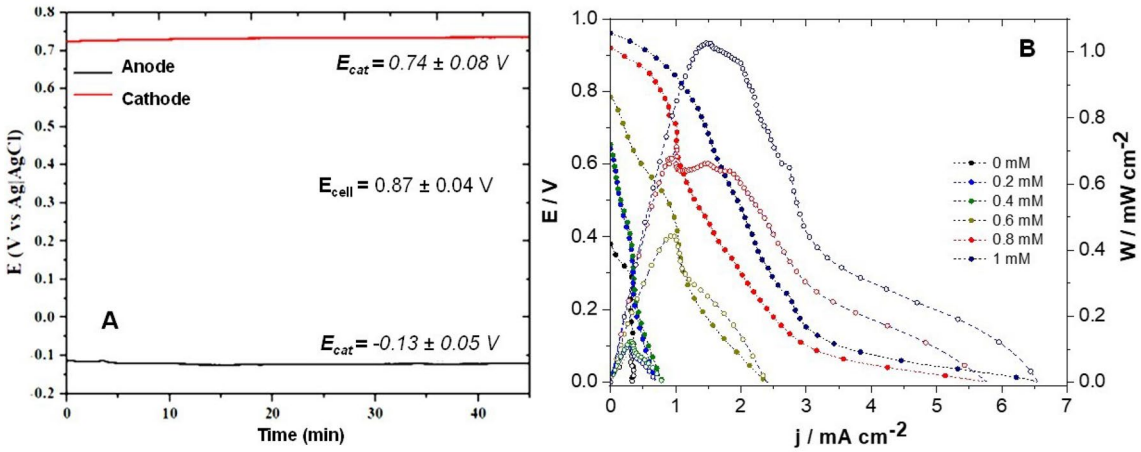

Fig. 5 **a** OCV in half-cell of Cu/Cu_2O-based anode in 0.1 M KOH and 0.4 mM Chol and cathode (Pt/C) in 0.5 M H_2SO_4; **b** power and current curves in a μFC obtained in the presence of different Chol concentrations: 0, 0.2, 0.4, 0.6, 0.8, 1 mM at 3 mL h^{-1} flow rate and 10 mV s^{-1} scan rate

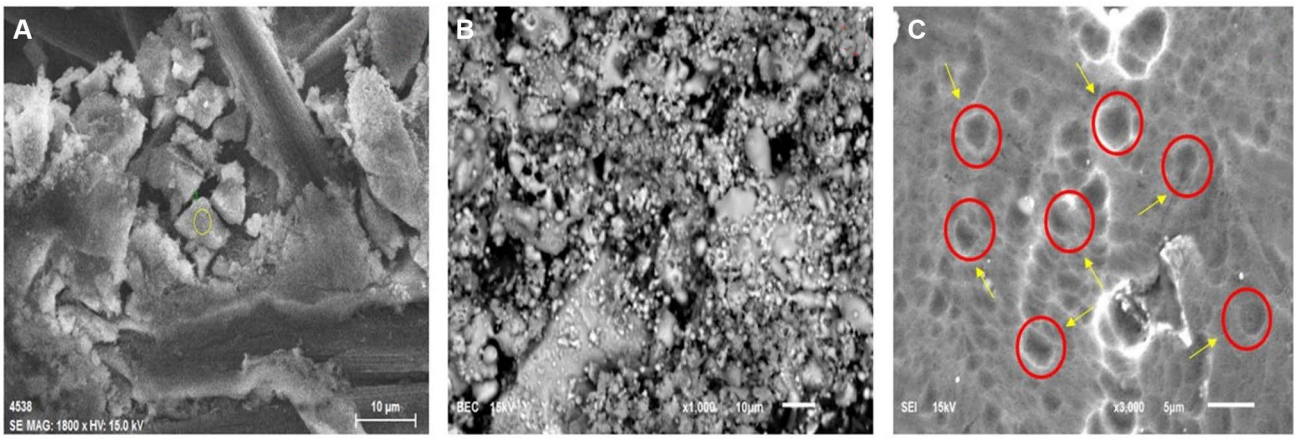

Fig. 6 **a** Electrode-modified Cu/Cu_2O NPs prior to use in µFC, **b** electrode modified with Cu/Cu_2O NPs after being used in cholesterol-based µFC, **c** electrode without catalyst used in µFC

as a possible cholesterol self-powered biosensor. However, additional tests need to be conducted to confirm this statement. It should be noted that this work, to the best of our knowledge, is the first microfluidic abiotic fuel cell using cholesterol as fuel. On the other hand, there are reports for microfluidic cholesterol biosensor [48].

In addition, a SEM analysis of the Cu/Cu_2O NPs was carried out, before (Fig. 6a) and after the NPs were used in the µFC (Fig. 6b). Figure 6b displays the Cu/Cu_2O electrode after being used in the µFC, where a type of granulation, possibly due presence of Triton X-100, is observed. In Fig. 6C, even adsorbed cholesterol could be appreciated.

The development of a cholesterol sensor and µFC is of great importance in the field of biomedicine and health for clinical analyses of cardiovascular diseases. Therefore, this device allows to sensitize cholesterol in a more effective and precise electrochemical way. Moreover, it provides energy through non-conventional fuels, creating a self-sustaining process. The sensor and the µFC based on Chol proposed in this research present advantages such as rapid response, small amount of sample intake, lower limit of detection, and high performance, providing energy from an unconventional and making for effective manufacturing and profitability.

Conclusions

This work presents a nanostructured material based on Cu/Cu_2O as a promising catalyst for cholesterol detection and oxidation reaction. By means of several physicochemical techniques, the composition, structure, morphology, and size parameters of Cu/Cu_2O-based material were characterized. The nanoparticles were used in a sensor and anodic material in a microfluidic fuel cell using cholesterol as a fuel. In the case of the cholesterol sensor, the LOD and LOQ values were smaller than those already reported with potential use for the quantification of cholesterol in biological fluids. Regarding the microfluidic fuel cell device, this device generated a voltage around to 0.96 V and 6.5 mA cm^{-2} and 1.03 mW cm^{-2} of current and power density, respectively, in the presence of low cholesterol concentration between 0.2 and 1 mM, without the need for oxygen saturation by air supply and, using optimal electrolyte conditions for the anolyte and catholyte. This reduces the cost of the device and electrodes by replacing of the enzymes by use of abundant and non-noble metal as cupper. Cu-based NPs presented an excellent performance for the dual application both microfluidic fuel cell and sensor with potential applications in biomedicine and as an alternative energy source.

Acknowledgements The authors would like to thank the Mexican Council for Science and Technology (CONACYT) for the financial support through the project *Ciencia de Frontera* Grant No. 845132, Chairs-CONACYT-Project Number 746 and the LABMYN 2022-321116 for the technical support. Estancia Sabática-CONACYT 202.

Declarations

Conflict of interest The authors declare that they have no conflict of interest.

References

1. Dumont, O., Frate, G.F., Pillai, A., Lecompte, S., Paepe, M.D., Lemort, V.: Carnot battery technology: a state-of-the-art review. J Energy Storage (2020). https://doi.org/10.1016/j.est.2020.101756
2. Weitzer, M., Müller, D., Steger, D., Charalampidis, A., Karellas, S., Karl, J.: Organic flash cycles in Rankine-based Carnot batteries with large storage temperature spreads. Energy Convers Manag **255**, 115323 (2022). https://doi.org/10.1016/j.enconman.2022.115323
3. Singh, R., Kaur, N., Singh, M.: Bio-compatible bio-fuel cells for medical devices. Mater Today Proc **44**, 242–249 (2021). https://doi.org/10.1016/j.matpr.2020.09.461
4. Nasar, A., Perveen, R.: Applications of enzymatic biofuel cells in bioelectronic devices—a review. Int J Hydrog Energy **44**, 15287–15312 (2019). https://doi.org/10.1016/j.ijhydene.2019.04.182
5. Wang, Y., Luo, S., Kwok, H.Y.H., Pan, W., Zhang, Y., Zhao, X., Leung, D.Y.C.: Microfluidic fuel cells with different types of fuels: a prospective review. Renew Sustain Energy Rev **141**, 110806 (2021). https://doi.org/10.1016/j.rser.2021.110806
6. Ibrahim, O.A., Navarro-Segarra, M., Sadeghi, P., Sabaté, N., Esquivel, J.P., Kjeang, E.: Microfluidics for electrochemical energy conversion. Chem Rev **122**, 7236–7266 (2022). https://doi.org/10.1021/acs.chemrev.1c00499
7. Shinohata, R., Shibakura, M., Arao, Y., Watanabe, S., Hirohata, S., Usui, S.: A high-fat/high-cholesterol diet, but not high-cholesterol alone, increases free cholesterol and apoE-rich HDL serum levels in rats and upregulates hepatic ABCA1 expression. Biochimie **197**, 49–58 (2022). https://doi.org/10.1016/j.biochi.2022.01.011
8. Komathi, S., Muthuchamy, N., Lee, K., Gopalan, A.: Fabrication of a novel dual mode cholesterol biosensor using titanium dioxide nanowire bridged 3D graphene nanostacks. Biosens Bioelectron **84**, 64–71 (2016). https://doi.org/10.1016/j.bios.2015.11.042
9. Arya, S.K., Datta, M., Malhotra, B.D.: Recent advances in cholesterol biosensor. Biosens Bioelectron **23**, 1083–1100 (2008). https://doi.org/10.1016/j.bios.2007.10.018
10. Chiang, W., Chen, P., Nien, P., Ho, K.: Amperometric detection of cholesterol using an indirect electrochemical oxidation method. Steroids **76**, 1535–1540 (2011). https://doi.org/10.1016/j.steroids.2011.09.003
11. Tee, S.Y., Teng, C.P., Ye, E.: Metal nanostructures for non-enzymatic glucose sensing. Mater Sci Eng C **70**, 1018–1030 (2017). https://doi.org/10.1016/j.msec.2016.04.009
12. Rewatkar, P., Hitaishi, V.P., Lojou, E., Goel, S.: Enzymatic fuel cells in a microfluidic environment: status and opportunities. A mini review. Electrochem commun **107**, 106533 (2019). https://doi.org/10.1016/j.elecom.2019.106533
13. Fornazier Filho, Y., da Cruz, A.C.C., Pedicini, R., Salgado, J.R.C., Luz, P.P., Ribeiro, J.: Development of palladium catalysts modified by ruthenium and molybdenum as anode in direct ethanol fuel cell. Mater Renew Sustain Energy **10**, 1–12 (2021). https://doi.org/10.1007/s40243-020-00187-1
14. Baronia, R., Goel, J., Kaswan, J., Shukla, A., Singhal, S.K., Singh, S.P.: PtCo/rGO nano-anode catalyst: enhanced power density with reduced methanol crossover in direct methanol fuel cell. Mater Renew Sustain Energy **7**, 1–13 (2018). https://doi.org/10.1007/s40243-018-0134-8
15. Gribov, E.N., Kuznetsov, A.N., Golovin, V.A., Krasnikov, D.V., Kuznetsov, V.L.: Effect of modification of multi-walled carbon nanotubes with nitrogen-containing polymers on the electrochemical performance of Pt/CNT catalysts in PEMFC. Mater Renew Sustain Energy **8**, 1–13 (2019). https://doi.org/10.1007/s40243-019-0143-2
16. Feng, Y., Xu, Y., Liu, S., Wu, D., Su, Z., Chen, G., Liu, J., Li, G.: Recent advances in enzyme immobilization based on novel porous framework materials and its applications in biosensing. Coord Chem Rev (2022). https://doi.org/10.1016/j.ccr.2022.214414
17. Hassan, N.: Catalytic performance of nanostructured materials recently used for developing fuel cells' electrodes. Int J Hydrog Energy **46**, 39315–39368 (2021). https://doi.org/10.1016/j.ijhydene.2021.09.177
18. Khaliq, N., Asim, M., Cha, G., Khan, M., Karim, S.: Chemical Development of non-enzymatic cholesterol bio-sensor based on TiO_2 nanotubes decorated with Cu_2O nanoparticles. Sens Actuators B Chem **302**, 127200 (2020). https://doi.org/10.1016/j.snb.2019.127200
19. Mulla, R., Rabinal, M.K.: CuO/CuxS composites fabrication and their thermoelectric properties. Mater Renew Sustain Energy **10**, 1–7 (2021). https://doi.org/10.1007/s40243-021-00189-7
20. Salazar, P., Martín, M., González-mora, J.L.: In situ electrodeposition of cholesterol oxidase-modified polydopamine thin film on nanostructured screen printed electrodes for free cholesterol determination. J Electroanal Chem **837**, 191–199 (2019). https://doi.org/10.1016/j.jelechem.2019.02.032
21. Barik, A., Dutta, J.C.: Fabrication and characterization of junctionless carbon nanotube field effect transistor for cholesterol detection Fabrication and characterization of junctionless carbon nanotube field effect transistor for cholesterol detection. Appl Phys Lett **053509**, 1–6 (2014). https://doi.org/10.1063/1.4892469
22. Khan, S., Rasheed, M.A., Shah, A., Mahmood, A., Waheed, A., Karim, S., Khan, M., Ali, G.: Preparation of oxidized Zn–In nanostructures for electrochemical non-enzymatic cholesterol sensing. Mater Sci Semicond Process **135**, 106101 (2021). https://doi.org/10.1016/j.mssp.2021.106101
23. Maya-Cornejo, J., Arjona, N., Guerra-Balcázar, M., Álvarez-Contreras, L., Ledesma-García, J., Arriaga, L.G.: Synthesis of Pd–Cu bimetallic electrocatalyst for ethylene glycol and glycerol oxidations in alkaline media. Procedia Chem **12**, 19–26 (2014). https://doi.org/10.1016/j.proche.2014.12.036
24. Wang, S., Chen, S., Shang, K., Gao, X., Wang, X.: Sensitive electrochemical detection of cholesterol using a portable paper sensor based on the synergistic effect of cholesterol oxidase and nanoporous gold. Int J Biol Macromol **189**, 356–362 (2021). https://doi.org/10.1016/j.ijbiomac.2021.08.145
25. Mir, I.A., Kumar, S., Bhat, M.A., Yuelin, X., Wani, A.A., Zhu, L.: Core@shell quantum dots as a fluorescent probe for the detection of cholesterol and heavy metal ions in aqueous media. Colloids Surf A Physicochem Eng Asp **626**, 127090 (2021). https://doi.org/10.1016/j.colsurfa.2021.127090
26. Ariyanta, H.A., Ivandini, T.A., Yulizar, Y.: Poly(methyl orange)-modified NiO/MoS2/SPCE for a non-enzymatic detection of cholesterol. FlatChem **29**, 100285 (2021). https://doi.org/10.1016/j.flatc.2021.100285
27. Escalona-Villalpando, R.A., Martínez-Maciel, A.C., Espinosa-Ángeles, J.C., Ortiz-Ortega, E., Arjona, N., Arriaga, L.G., Ledesma-García, J.: Evaluation of hybrid and enzymatic nanofluidic fuel cells using 3D carbon structures. Int J Hydrog Energy (2018). https://doi.org/10.1016/j.ijhydene.2018.04.016
28. Colicchio, I., Wen, F., Keul, H., Simon, U., Moeller, M.: Sulfonated poly(ether ether ketone)-silica membranes doped with phosphotungstic acid. Morphology and proton conductivity. J Memb Sci **326**, 45–57 (2009). https://doi.org/10.1016/j.memsci.2008.09.008
29. Alves, D.C.B., Silva, R., Voiry, D., Asefa, T., Chhowalla, M.: Copper nanoparticles stabilized by reduced graphene oxide for CO_2 reduction reaction. Mater Renew Sustain Energy (2015). https://doi.org/10.1007/s40243-015-0042-0
30. Iqbal, K., Ikram, M., Afzal, M., Ali, S.: Efficient, low-dimensional nanocomposite bilayer CuO/ZnO solar cell at various annealing

temperatures. Mater. Renew. Sustain. Energy. **7**, 1–7 (2018). https://doi.org/10.1007/s40243-018-0111-2
31. Hosokawa, Y., Hakamata, H., Murakami, T., Aoyagi, S., Kuroda, M.: Electrochemical oxidation of cholesterol in acetonitrile leads to the formation of cholesta-4, 6-dien-3-one. Electrochim Acta **54**, 6412–6416 (2009). https://doi.org/10.1016/j.electacta.2009.06.005
32. Kumar, P., Verma, N.: Electrochemically deposited dendritic poly (methyl orange) nano fi lm on metal-carbon-polymer nanocomposite: a novel non-enzymatic electrochemical biosensor for cholesterol Cu/Ni-nitrates-ACF electro-polymerization of PVAc+NaOH mixing and casting P. J Electroanal Chem **814**, 134–143 (2018). https://doi.org/10.1016/j.jelechem.2018.02.011
33. Ansari, A.A., Malhotra, B.D.: Current progress in organic—inorganic hetero-nano-interfaces based electrochemical biosensors for healthcare monitoring. Coord Chem Rev **452**, 214282 (2022). https://doi.org/10.1016/j.ccr.2021.214282
34. Thieu, N.A.T., Vu, M.C., Lee, E.S., Doan, V.C., Kim, S.R.: Enhancement of thermal conductivity of poly(methylmethacrylate) composites at low loading of copper nanowires. Macromol Res **27**, 1117–1123 (2019). https://doi.org/10.1007/s13233-019-7155-8
35. Chandrasekar, A., Vasantharaj, S., Jagadeesan, N.L., Shankar, S.N., Pannerselvam, B., Bose, V.G., Arumugam, G., Shanmugavel, M.: Studies on phytomolecules mediated synthesis of copper oxide nanoparticles for biomedical and environmental applications. Biocatal Agric Biotechnol **33**, 101994 (2021). https://doi.org/10.1016/j.bcab.2021.101994
36. Yuan, B., Xu, C., Liu, L., Zhang, Q., Ji, S., Pi, L., Zhang, D., Huo, Q.: Cu2O/NiOx/graphene oxide modified glassy carbon electrode for the enhanced electrochemical oxidation of reduced glutathione and nonenzyme glucose sensor. Electrochim Acta **104**, 78–83 (2013). https://doi.org/10.1016/j.electacta.2013.04.073
37. Rasmussen, M., Abdellaoui, S., Minteer, S.D.: Enzymatic biofuel cells: 30 years of critical advancements. Biosens Bioelectron **76**, 91–102 (2016). https://doi.org/10.1016/j.bios.2015.06.029
38. Ji, R., Wang, L., Wang, G., Zhang, X.: Synthesize thickness copper (I) sulfide nanoplates on copper rod and it's application as nonenzymatic cholesterol sensor. Electrochim Acta **130**, 239–244 (2014). https://doi.org/10.1016/j.electacta.2014.02.155
39. Kunwar, A., Hektor, J., Nomoto, S., Coutinho, Y.A., Moelans, N.: Combining multi-phase field simulation with neural network analysis to unravel thermomigration accelerated growth behavior of Cu6Sn5 IMC at cold side Cu–Sn interface. Int J Mech Sci **184**, 105843 (2020). https://doi.org/10.1016/j.ijmecsci.2020.105843
40. Tong, Y., Li, H., Guan, H., Zhao, J., Majeed, S., Anjum, S., Liang, F., Xu, G.: Electrochemical cholesterol sensor based on carbon nanotube@molecularly imprinted polymer modified ceramic carbon electrode. Biosens Bioelectron **47**, 553–558 (2013). https://doi.org/10.1016/j.bios.2013.03.072
41. Joshi, N., Sharma, A., Asokan, K., Rawat, K., Kanjilal, D.: Effect of hydrogen ion implantation on cholesterol sensing using enzyme-free LAPONITE®-montmorillonite electrodes. RSC Adv **6**, 22664–22672 (2016). https://doi.org/10.1039/C5RA27523G
42. Li, L., Wang, Y., Pan, L., Shi, Y., Cheng, W., Shi, Y., Yu, G.: A nanostructured conductive hydrogels-based biosensor platform for human metabolite detection. Nano Lett **15**, 1146–1151 (2015). https://doi.org/10.1021/nl504217p
43. Gao, J., Huang, W., Chen, Z., Yi, C., Jiang, L.: Simultaneous detection of glucose, uric acid and cholesterol using flexible microneedle electrode array-based biosensor and multi-channel portable electrochemical analyzer. Sens Actuators B Chem **287**, 102–110 (2019). https://doi.org/10.1016/j.snb.2019.02.020
44. Escalona-Villalpando, R.A., Reid, R.C., Milton, R.D., Arriaga, L.G., Minteer, S.D., Ledesma-García, J.: Improving the performance of lactate/oxygen biofuel cells using a microfluidic design. J Power Sour (2017). https://doi.org/10.1016/j.jpowsour.2016.12.082
45. Moreno-Zuria, A., Ortiz-Ortega, E., Gurrola, M.P., Chávez-Ramírez, A.U., Ledesma-García, J., Arriaga, L.G.: Evolution of microfluidic fuel stack design as an innovative alternative to energy production. Int J Hydrog Energy **42**, 27929–27939 (2017). https://doi.org/10.1016/j.ijhydene.2017.05.185
46. Quah, T., Abdellaoui, S., Milton, R.D., Hickey, D.P., Minteer, S.D.: Cholesterol as a promising alternative energy source: bioelectrocatalytic oxidation using NAD-dependent cholesterol dehydrogenase in human serum. J Electrochem Soc **164**, H3024–H3029 (2017). https://doi.org/10.1149/2.0021703jes
47. Sekretaryova, A.N., Beni, V., Eriksson, M., Karyakin, A.A., Turner, A.P.F., Vagin, M.Y.: Cholesterol self-powered biosensor. Anal Chem **86**, 9540–9547 (2014). https://doi.org/10.1021/ac501699p
48. Kaur, G., Tomar, M., Gupta, V.: Sensors and actuators B: chemical development of a microfluidic electrochemical biosensor: prospect for point-of-care cholesterol monitoring. Sens Actuators B Chem **261**, 460–466 (2018). https://doi.org/10.1016/j.snb.2018.01.144